

**Final report on ALMA Development Study 445**  
**DEVELOPMENT OF SECOND-GENERATION**  
**SIS RECEIVERS FOR ALMA**

A. R. Kerr, J. G. Mangum, J. E. Effland, P. Dindo, S. Srikanth  
NRAO

A. W. Lichtenberger  
University of Virginia

31 October 2017

**Summary:** This report describes work done towards a new generation of SIS receivers for ALMA under ALMA Study 445 over the period 1 October 2016 to 30 September 2017. The following summarizes the work done under this proposal:

1. Towards second generation SIS mixers for ALMA Bands 6-10.
  - (a) High quality Nb/Al-AlN/Nb SIS junctions with high critical current density ( $J_c$ ) have been produced which are suitable for Bands 6-8. All current ALMA SIS mixers have Nb/Al-AlOx/Nb junctions, which do not have a high enough  $J_c$  to give flat receiver gain and noise temperature across the full ALMA RF bands.
  - (b) A process has been developed for making high quality NbTiN, which has a higher energy gap than Nb and is suitable for future SIS mixers in Bands 9 and 10. Good quality SIS junctions have been made with one or both electrodes made of NbTiN, and with AlN tunnel barriers for high  $J_c$ . These have not yet been tested in SIS mixers.
2. A wideband (4-12 GHz) balanced IF amplifier small enough to replace the IF amplifiers in the current ALMA SIS receivers (*i.e.*, Bands 3 to 10) has been designed. Such a wideband amplifier will be necessary to take advantage of the planned correlator upgrade which will be able to handle 32 GHz of bandwidth (2 polarizations x 2 sidebands x 8 GHz).
  - (a) To meet the stringent power limitations of the ALMA receivers, the balanced amplifiers must dissipate no more than 8.5 mW each.
  - (b) The noise temperature of the balanced amplifiers at mid-band must be no greater than that of the current IF amplifiers, including isolators in the bands where they are used, and should be flat across the full 4-12 GHz IF band.
  - (c) The amplifiers must be small enough that four of them can be mounted on the 4-K stage of the cartridges. This precludes the use of standard coupled stripline quadrature hybrids which are too large. Instead, a superconducting quasi-lumped element hybrid on a small chip has been designed and tested.
3. An improved orthomode transducer (OMT) and feed horn have been designed and simulated. Goals:
  - (a) Remove trapped mode resonance present in current Band-6 horn-OMT assembly.
  - (b) Reduce sidelobe level.
  - (c) Improve OMT design to give easier assembly and better repeatability.

## 1. Second generation SIS mixers for ALMA Bands 6 and 10

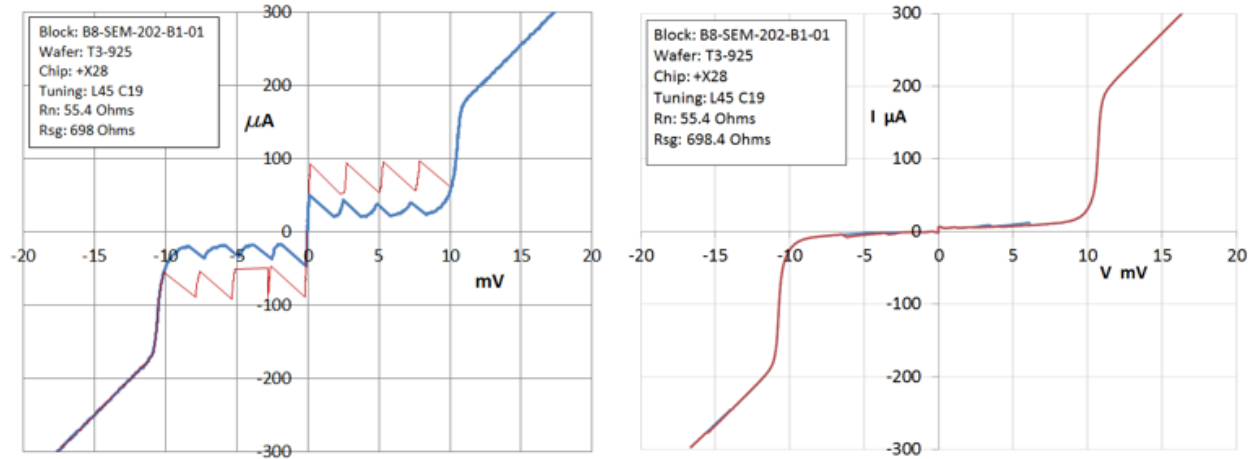
A key to the next generation of SIS mixers will be aluminum nitride (AlN) tunnel barriers. With electrodes of niobium, niobium nitride, or both, SIS junctions with AlN tunnel barriers can be made with greater critical current density ( $J_c$ ) than those with the standard  $\text{Al}_2\text{O}_3$  barriers. For a given normal resistance this allows smaller-area junctions with lower capacitance which will allow the next generation of SIS receivers to have a much flatter noise temperature across their full RF band.

For SIS receivers above  $\sim 600$  GHz (ALMA Bands 9 and 10), Nb RF circuits are not suitable because of their loss. NbTiN, with its higher energy gap is preferable in this frequency range.

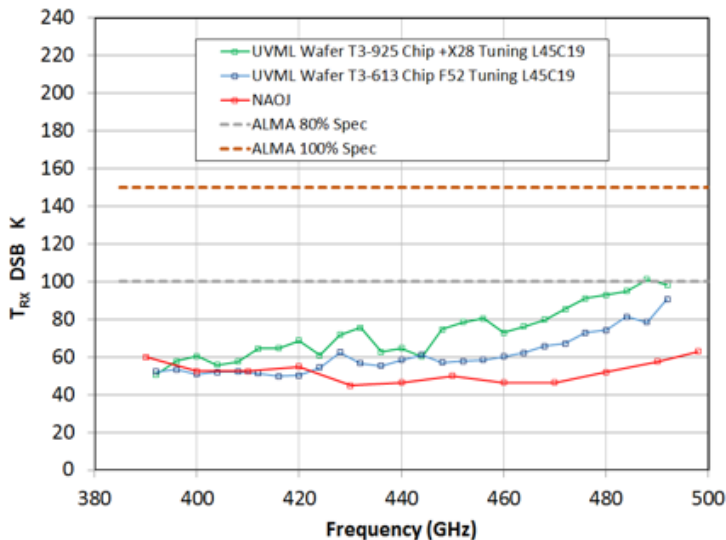
### Qualifying AlN tunnel barriers

The goal of this study was to work towards high quality Nb/Al-AlN/Nb SIS junctions for ALMA Band 6 and NbTiN/Al-AlN/Nb or NbTiN/AlN/NbTiN junctions for ALMA Band 10. As an initial step, we wanted to demonstrate that an AlN tunnel barrier would give SIS receivers with as low noise temperature as those with  $\text{Al}_2\text{O}_3$  barriers (as used at present in ALMA's SIS receivers). Since SIS junctions with NbTiN electrodes were not available at the beginning of this study, tests of AlN barriers were done with Nb/Al-AlN/Nb junctions at half the Band 10 frequency, 385-500 GHz.

Fig. 1.1 shows the  $I(V)$  characteristics of a series array of four Nb/Al-AlN/Nb junctions used in a 385-500 GHz receiver. Fig. 1.2 shows the receiver noise temperature as a function of LO frequency for two mixers from different wafers and also for an ALMA Band 8 mixer (Nb/Al- $\text{Al}_2\text{O}_3$ /Nb junctions). The numbers are similar at the low frequency end of the band, but rise significantly at the upper end, indicating that the new mixer is tuned too low in frequency. *The fact that*



Above: Fig. 1.1  $I(V)$  characteristic of a Nb/Al-AlN/Nb SIS mixer with four junctions in series. Nominal diameter  $1.0 \mu\text{m}$ ,  $J_c = 20,000 \text{ A/cm}^2$  and  $R_N = 45 \Omega$ . Left plot:  $I(V)$  curves with no applied magnetic field:  $|V|$  increasing (red) and  $|V|$  decreasing (blue). Right plot:  $I(V)$  curve with magnetic field adjusted to suppress Josephson currents.



Left: Fig. 1.2 DSB noise temperatures of 385 GHz SIS receivers. Blue: wafer T3-613. Green: wafer T3-925. The red curve is for an ALMA Band-8 receiver.

the noise temperatures for the mixers with AlN barriers are comparable with those for the  $Al_2O_3$  barriers over the lower part of the band demonstrates that there is no additional source of noise associated with the AlN barriers.

#### Precise control of AlN barrier thickness

Prior to the current work, it was difficult to control the thickness of the AlN barrier of SIS junctions, and hence  $J_C$ . The nitridation process was too rapid in the Inductively Coupled Plasma system and too thick a layer would grow in only a few seconds. Nevertheless, the junction quality at high  $J_C$  was good as seen in Fig. 1.3. Consequently, the ICP system was modified by adding a spacer in the vacuum system between the source and the target to reduce the nitridation rate. Fig. 1.4 shows the AlN thickness vs time before and after the modification. Characteristics of SIS junctions made with the modified system have not yet been measured.

**Fig. 1.3**  $I(V)$  characteristic of a Nb/Al-AlN/Nb SIS junction of diameter  $0.98\ \mu\text{m}$  and with  $J_C = 18\ \text{kA/cm}^2$ .

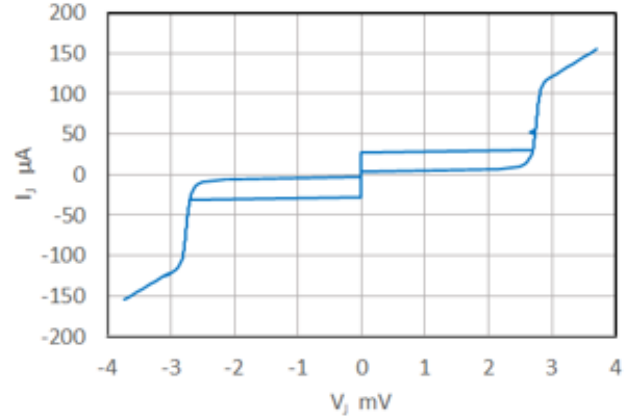
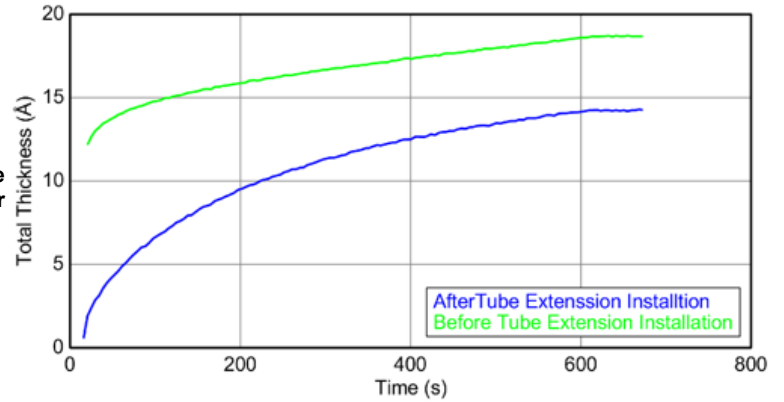


**Fig. 1.4** AlN thickness vs time, before modification of the ICP system (green) and after (blue).



#### SIS junctions with NbTiN electrodes

NbTiN is well suited for use in SIS mixers above  $\sim 600\ \text{GHz}$ . With its higher energy gap, it should make SIS mixers with quantum-limited sensitivity to well over  $1\ \text{THz}$ . Following UVML's earlier success making Nb/Al-AlN/NbTiN junctions [1.1], recent work has focused on making all-NbTiN SIS junctions (NbTiN/AlN/NbTiN) with AlN tunnel barriers deposited using Reactive Bias Target Ion Beam Deposition (RBTIBD), which offers more control over film quality than conventional magnetron deposition. Fig. 1.5 shows the  $I(V)$  characteristics of experimental NbTiN/AlN/NbTiN junctions made in this way. Note the high gap voltage:  $5\ \text{mV}$  for NbTiN/AlN/NbTiN compared with  $2.8\ \text{mV}$  for Nb/Al-AlN/Nb (as in Fig. 1.3). The  $J_C$  dependence on AlN deposition time for NbTiN/AlN/NbTiN junctions made in the RBTIBD system is shown in Fig. 1.6.

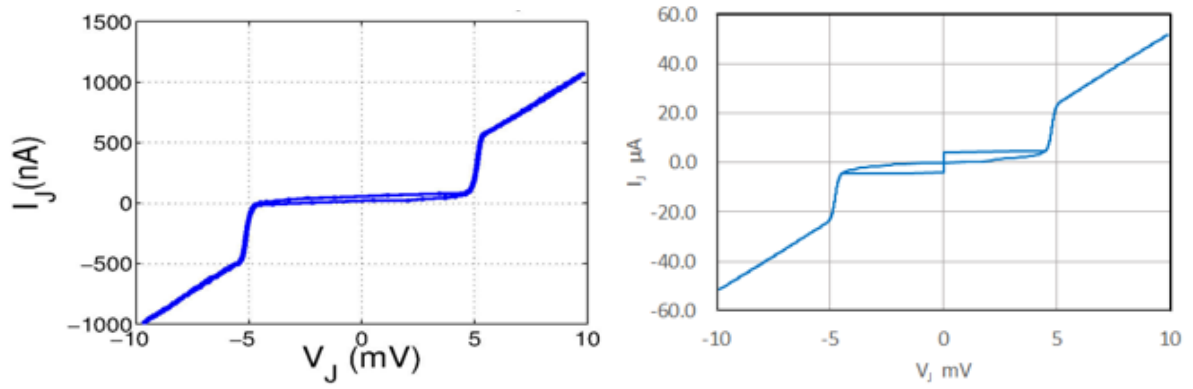


Fig. 1.5  $I(V)$  characteristics of experimental NbTiN/AlN/NbTiN SIS junctions. Note the high gap voltage  $V_g \approx \sim 5$  mV. Left: Junction diameter  $2.1 \mu\text{m}$ , and very low  $J_c = 12.7 \text{ A/cm}^2$ . Right: Junction diameter  $1.2 \mu\text{m}$  and  $J_c = 2,000 \text{ A/cm}^2$ .

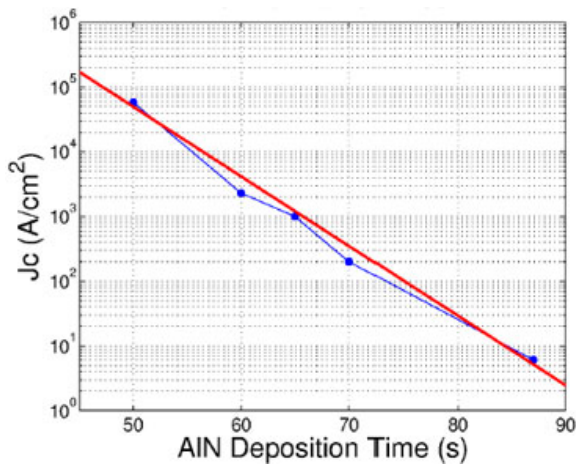


Fig. 1.6 Critical current density ( $J_c$ ) as a function of AlN deposition time for NbTiN/AlN/NbTiN SIS junctions, after modifying the RBTIBD system.

## 2. Wideband (4-12 GHz) balanced IF amplifier

### *Choice of IF band*

With the planned correlator upgrade, ALMA will be able to handle twice its present instantaneous bandwidth. Currently only 4 GHz of IF bandwidth per sideband per polarization (16 GHz total) can be processed, but with the new correlator that will increase to 8 GHz per sideband per polarization (32 GHz total). There has been considerable discussion about the merits of increasing the IF taking into account the particular molecular species which could be observed simultaneously with a higher and/or wider IF, and the noise penalty of using a higher IF – see [2.1] and [2.2]. The conclusions are that: (i) the IF should extend down to 4 GHz to allow the  $^{12}\text{CO}$  and  $^{13}\text{CO}$  lines at 220 and 230 GHz to be observed simultaneously; (ii) with the new correlator there will be no advantage in increasing the IF bandwidth beyond 8 GHz; and (iii) changing to a substantially higher IF would impose a significant noise penalty. For the foreseeable future the preferred IF band will be 4-12 GHz.

### *Balanced IF amplifiers*

The current ALMA SIS receivers (Bands 3-10) all use HFET IF amplifiers operating at 4 K. With the exception of Band 6, all use ferrite IF isolators which add to the receiver noise temperature. Most bands currently use a 4-8 GHz IF. A balanced amplifier based on the latest MMICs from Low Noise Factory would allow all bands of ALMA to be upgraded to the preferred 4-12 GHz IF, and isolators would not be needed. For Band 6, which does not use IF isolators, balanced IF amplifiers will eliminate the slow variation of gain and noise temperature across the IF band caused in the present receivers by the interaction between the mixer and the preamp.

The balanced amplifier has long been used in the microwave industry for its inherently low input and output reflection coefficients. It has many of the characteristics of an amplifier preceded by a ferrite isolator, but potentially wider bandwidth. A noise analysis of the balanced amplifier [2.3] shows that its input and output noise waves are uncorrelated. This means that when connected to the output of a poorly matched SIS mixer, the electrical length of the connection will not cause gain or noise ripples across the amplifier band. Until recently, balanced amplifiers would not have been possible for use on ALMA because of their size and power dissipation. Because a balanced amplifier has two identical amplifiers in parallel, the power dissipation is twice that of the single amplifier. For ALMA receivers, the maximum allowed power dissipation of the IF amplifiers in any cartridge is 34 mW in total – for two polarizations with sideband-separating mixers that limits the dissipation of each amplifier to 8.5 mW. Only recently have such amplifiers become available. For balanced amplifiers with conventional stripline quadrature hybrids [2.4], the hybrids take up most of the

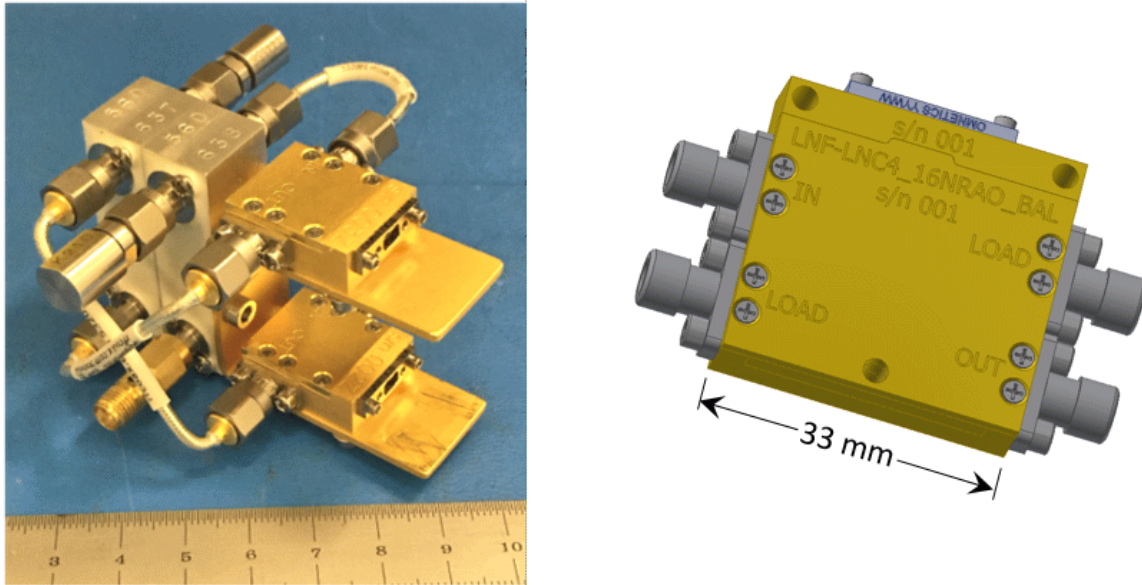


**Fig. 2.1 (Left) Photograph of a balanced 4-12 GHz amplifier using discrete amplifiers (gold) and hybrids (aluminum). The ruler is in cm. (Right) Image of the proposed balanced amplifier containing two superconducting quadrature hybrids, two MMIC amplifiers, and SIS mixer bias-T.**

volume. To reduce the size of the balanced amplifier we proposed using superconducting quasi-lumped element quadrature hybrids which could be made on a small 3 x 1 mm quartz chip. Fig 2.1 shows a conventional 4-12 GHz balanced amplifier composed of two stripline hybrids and two Low Noise Factory amplifiers, and the proposed balanced amplifier with two superconducting hybrids, two MMIC amplifiers, and an SIS mixer bias-T in a single package.

#### *4-12 GHz quadrature hybrid*

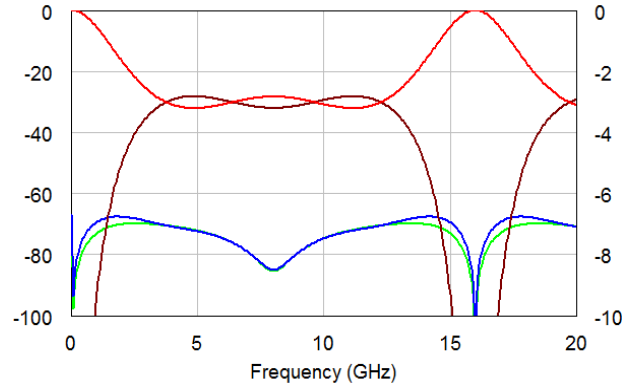
The concept of a superconducting lumped-element hybrid was successfully used for a 4-12 GHz 180° hybrid in 2006 [2.5][2.6]. That design was simpler than the present 90° design in that it used only lumped-element transmission lines, modeled by multiple series L and shunt C elements and a negative transmission line modeled by series C and shunt L elements. The 90° hybrid requires elements with both self and mutual inductance which are more difficult to design.

The design starts from a standard TEM coupled-line prototype using the prototype element values given in Table 13.03-1 of [2.7] for a hybrid with three quarter-wave sections and  $\pm 0.2$ dB ripple. For a 50-ohm characteristic impedance, the even- and odd-mode characteristic impedances of the three sections are as shown in the table:

Stage	Z <sub>oe</sub>	Z <sub>oo</sub>
1	60.2	41.5
2	169.8	14.7
3	60.2	41.5

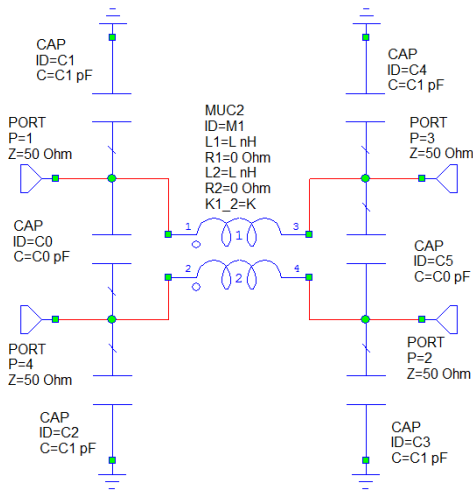
The S-parameters are shown in Fig. 2.2.

**Fig. 2.2 Characteristics of a TEM coupled-line hybrid with three quarter-wave sections and  $\pm 0.2$  dB passband ripple. Red and brown curves are  $S_{31}$  and  $S_{41}$  (dB, right axis); Blue and Green curves are  $S_{11}$  and  $S_{21}$  (dB, left axis).**



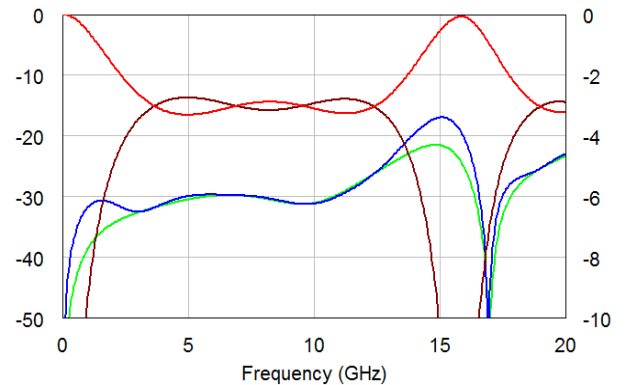
For the lumped-element hybrid, each quarter-wave section is approximated by a lumped-element equivalent circuit. Just as an incremental length of TEM transmission line can be represented by a series L and a shunt C element, an incremental length of a pair of coupled TEM lines can be represented by L, C, and M elements, M being the mutual inductance between two inductors, as shown in Fig. 2.3. For the quadrature hybrid we found that this equivalent circuit could

**Fig. 2.3. Equivalent circuit of an incremental length of a pair of coupled TEM lines. The inductors have self- and mutual-inductance.**



represent one twelfth of a wavelength of coupled lines with sufficient accuracy; hence each quarter-wave section of the hybrid is represented by three sections like Fig. 2.3 – a total of nine sections for the full three section hybrid. The optimizer in Microwave Office was used to fit the lumped-element circuits to the desired quarter-wave coupled TEM lines. Fig 2.4 shows the S-parameters of the resulting lumped-element model. In comparison with Fig. 2.2, it is clear that the lumped element is sufficiently accurate over the 4-12 GHz band.

**Fig. 2.4. Characteristics of the lumped-element model of the TEM coupled-line hybrid with three quarter-wave sections and  $\pm 0.2$  dB passband ripple. Red and brown curves are  $S_{31}$  and  $S_{41}$  (dB, right axis); Blue and Green curves are  $S_{11}$  and  $S_{21}$  (dB, left axis).**



The next step is to design superconducting circuits which match the two optimized lumped-element circuits. To achieve the required self and mutual inductance, overlapping planar spiral inductors are located on different layers of the circuit,



separated by 285 nm films of  $\text{SiO}_2$ . The final designs are shown in Fig. 2.5. Details are given in the figure caption. The surface inductance of the niobium superconductors is independent of frequency and has a small but significant effect. It is taken into account in the Sonnet simulations as described in [2.8].

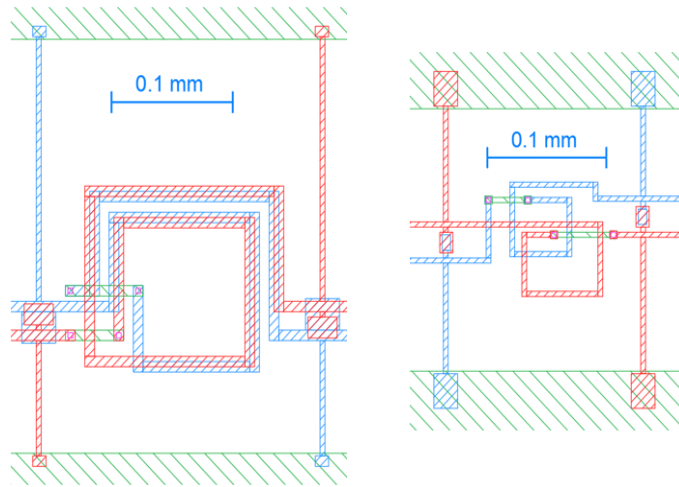


**Fig. 2.5. The two basic circuit elements of the hybrid. The substrate is fused quartz ( $K = 3.8$ ). The three conductor layers are separated by 285 nm  $\text{SiO}_2$  insulator layers. Conductors: red – Nb bottom layer; green – Nb middle layer (ground plane and some interconnections); blue – Nb top layer. Required additional capacitance between the layers is added by the parallel plate capacitors.**

Fig. 2.6 shows the complete hybrid chip with the bonding pads in the four corners connected to the hybrid circuit by 50-ohm capacitively loaded coplanar waveguides (CLCPW) as described in [2.9]. An isometric view of part of the hybrid is shown in Fig. 2.7, greatly expanded in the vertical direction to show details of the via connections between layers. Details of the bonding pad and CLCPW lines are shown in Fig. 2.8

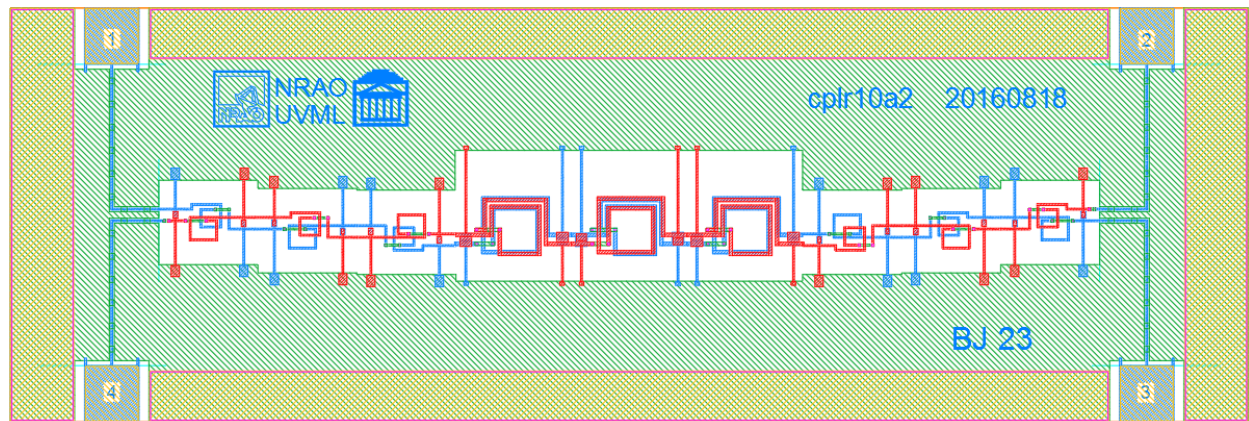


**Fig. 2.6 The complete superconducting 4-12 GHz quadrature hybrid on a fused quartz chip. The overall dimensions are 3 x 1 x 0.25 mm. On the top side of the quartz substrate there are three Nb layers (red, green, blue) separated by 285 nm layers of  $\text{SiO}_x$  ( $\epsilon_r = 3.9$ ). The border and the four bonding pads are gold (yellow) to allow wire bonding.**

Fig. 2.7 Isometric view of part of the hybrid, greatly expanded in the vertical direction to show details of the via connections between layers.

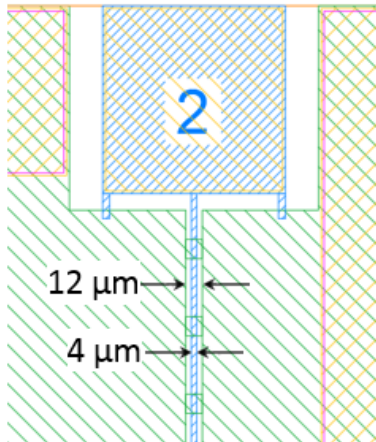
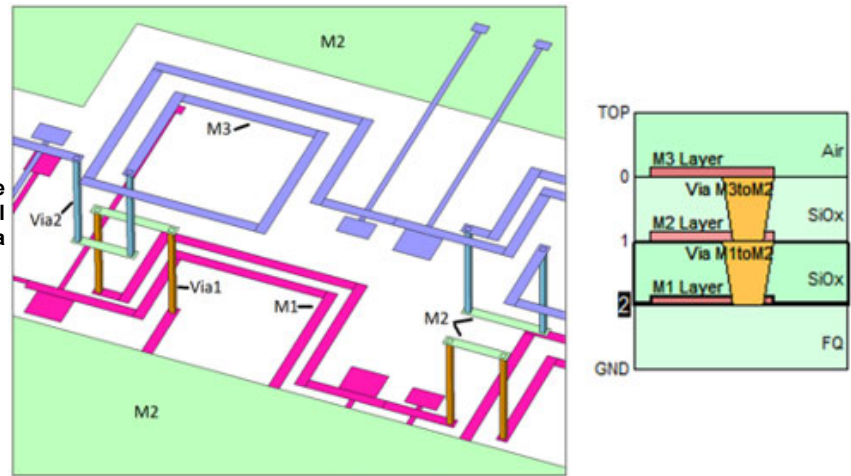


Fig. 2.8 Details of a CLCPW line and bonding pad [2.9]. The small tabs at the bottom of the bonding pad add capacitance to maintain a 50-Ω characteristic impedance from the bonding pad to the CLCPW.

#### Quadrature hybrid measurements

Two wafers of quadrature hybrids were fabricated at UVML, and at the time of writing a third wafer has been delivered but not yet tested. Fig. 2.9 shows the layout of the 50-mm quartz wafer. It contains 432 hybrids. To allow for processing variations, there are three slightly different designs on the wafer. After fabrication of a wafer at UVML, the wafers are probed for DC continuity between ports 1 & 3 and 2 & 4, and isolation between the ports 1 & 2 and 3 & 4. Most of the circuits on the first two wafers had one or more vias with high resistance. At 4-K, the vias had (I/V) characteristics similar to those of a weak-link Josephson junction, evidence that an oxide barrier was present in the via. The processing has been changed to eliminate this possibility in future.

A liquid helium cryostat with a large 4-K stage, made by Infrared Laboratories, was used for initial testing. It is shown in Fig. 2.10. This dewar was destroyed when a heater was left on too long after a cool-down, and a new test system using a closed-cycle Gifford-McMahon 4-K refrigerator has now been completed as a replacement. The 4-K working space is similar to that of the old cryostat.



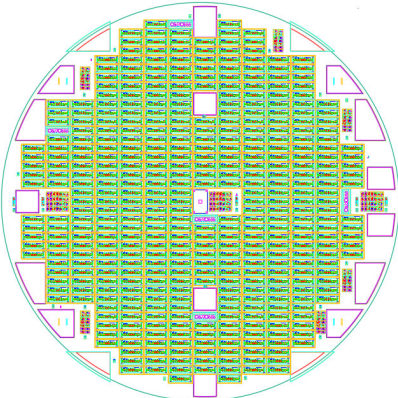


**Fig. 2.9** A 50-mm wafer of superconducting hybrids. A wafer contains 432 hybrids which have three tuning configurations to accommodate processing variations. The diagram is close to the actual size.

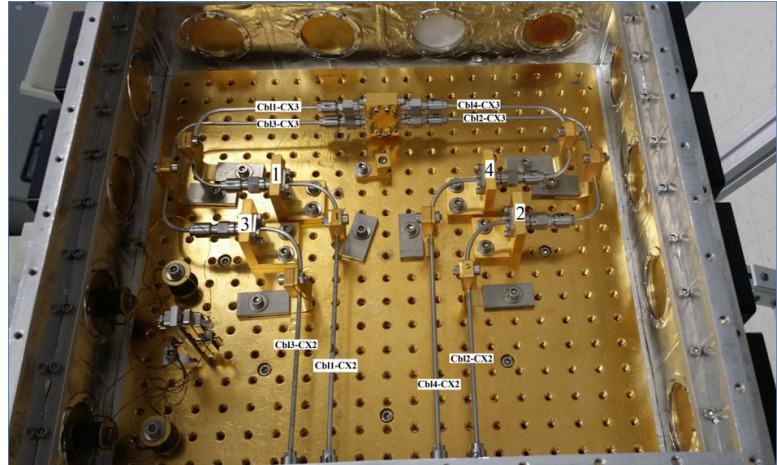


**Fig. 2.10** The Infrared Laboratories liquid helium cryostat with its cables and heatinks. 2.92-mm coaxial connectors are used throughout.

The hybrids were mounted in a test fixture with four 2.92-mm connectors as shown in Fig. 2.11. Microstrip lines on the 10-mil RT/duroid 6002 substrate connect the connectors to the hybrid chip. By changing the bondwires on the substrate,

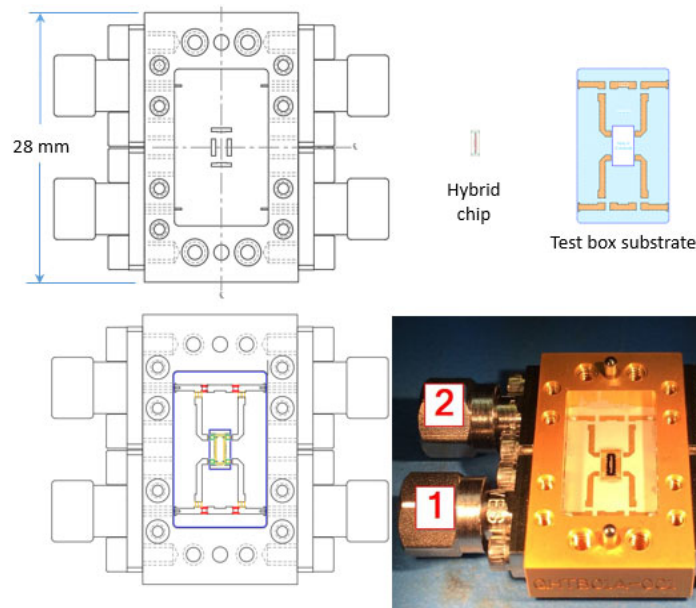


**Fig. 2.11** Details of the Hybrid test box. The 3 x 1 mm hybrid chip is mounted in the nest at the center of the box (top left diagram). Microstrip lines on the substrate connect to the chip. For hybrid measurements, the red bondwires (bottom left diagram) are removed. For circuit verification the yellow bondwires are removed.

the hybrid can be switched out of the circuit, allowing through measurement to be made between ports 1 & 4 and 2 & 3, to verify the characteristic impedance of the microstrip lines and the reflection coefficient of the connections.

VNA calibration is done in two steps. First a normal SOLT calibration is done at the ends of the test cables between the VNA and the external connectors on the cryostat. Then an identical hybrid test box, without a hybrid and with short-circuits to ground at the hybrid terminals, is cooled to 4 K and the Keysight Automatic Fixture Removal process used to move the reference planes to the short-circuit locations and to correct for loss and reflections in the cables from the cryostat wall to the new reference planes.

Measured S-parameters for two hybrids are shown in Fig. 2.12. Many of the hybrids on the first two wafers were found to have an excess resistance of several ohms in the vias between layers. As each path has 10 vias, the effect on the coupler performance is great. The via fabrication process was modified and a new wafer has been delivered, but not yet measured.

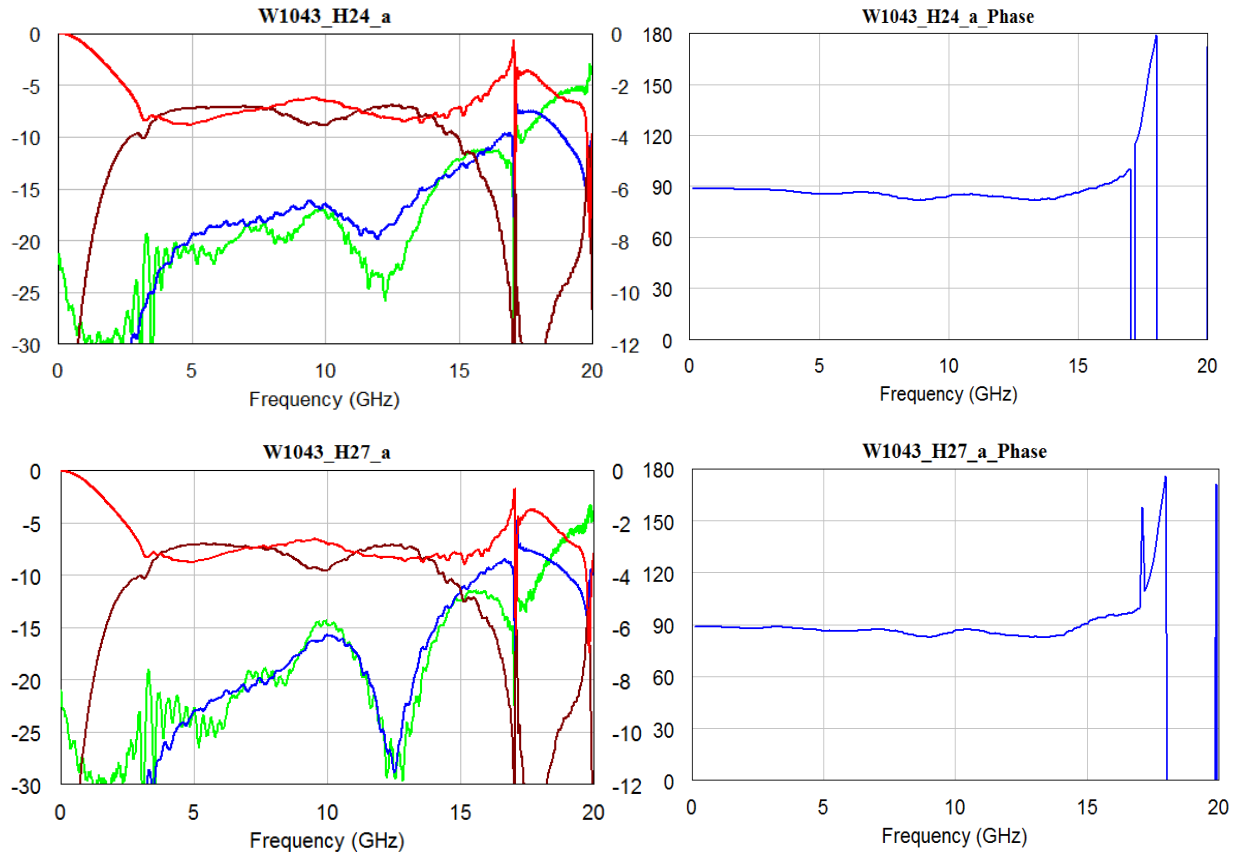


**Fig. 2.12 Measured S-parameters of 4-12 GHz superconducting quadrature hybrids H24 and H27. Box resonances are apparent above 17 GHz, but are of no consequence as they are above the band of interest.**

**Left plots (dB): red – through port; brown – coupled port; blue – isolated port; green – S11.**

**Right plots (degrees): phase difference between through and coupled ports.**

### 3. OMT and feed horn

The Bøifot junction orthomode transducer currently used in the Band 6 cartridges has wires in the side-arm ports that provide a low impedance path for main-arm wall currents. The main arm has a thin septum that separates the two ports of the main arm and also forms a pair of back-to-back “mitered” bends that feed the side-arm ports. Precise positioning of the wires and septum in the OMT assembly is critical to the performance, particularly the polarization properties. A new OMT by Dunning et al. [3.1] looks favorable for a Band-6 upgrade in terms of simplicity, ease of fabrication, and polarization performance.

The Dunning OMT is a simple split-block design and does not have the wires or septum required in the Bøifot OMT. It consists of an input section, a polarization separating junction, and an output section for each polarization. The geometry is shown in Fig. 3.1. The input section has a square input matched to the feed horn waveguide. The square section is then reduced to a smaller square waveguide, followed by a transition to a T-shaped cross-section waveguide. The polarization-separating junction removes one polarization via a mitered bend and allows the other to pass through. The transition from square to T-waveguide limits the useful bandwidth to 1.3:1, which is sufficient to cover ALMA Band 6.

Fig. 3.2 shows the measured S-parameters of a WR-10 version of the original Dunning OMT. It is well matched and has good isolation over the 1.3:1 frequency band indicated by the markers. However, we found that the polarization isolation is very sensitive to small misalignments between the block halves; this is shown in Fig. 3.3 (left).

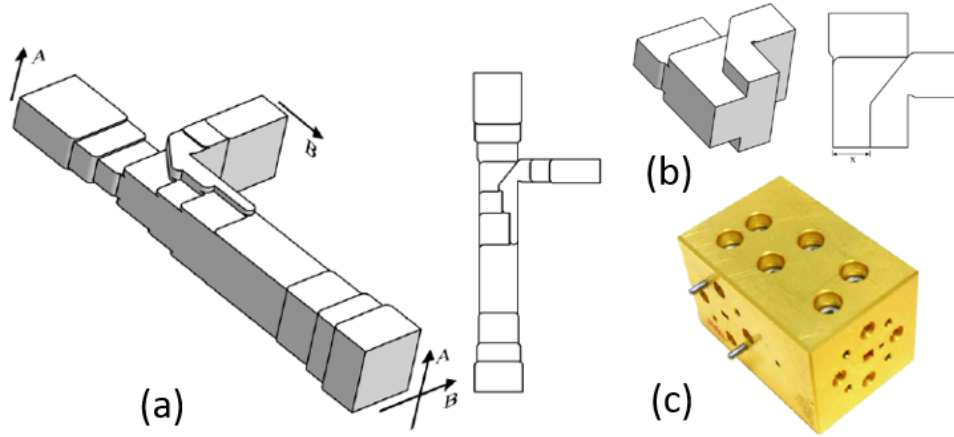


Fig. 3.1 The Dunning OMT can be machined as a simple split-block assembly [3.1].

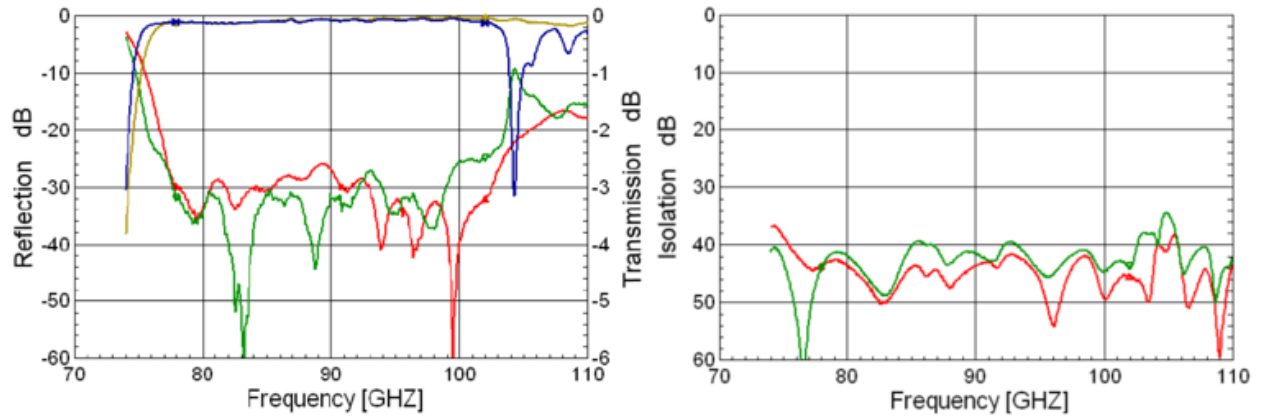


Fig. 3.2 Measured S-parameters of the OMT. Left: Transmission (side port blue, through port brown) and reflection coefficient (side arm green, through arm red) at the rectangular waveguide ports. Right: Isolation (side-port red, through-port green). [3.1]

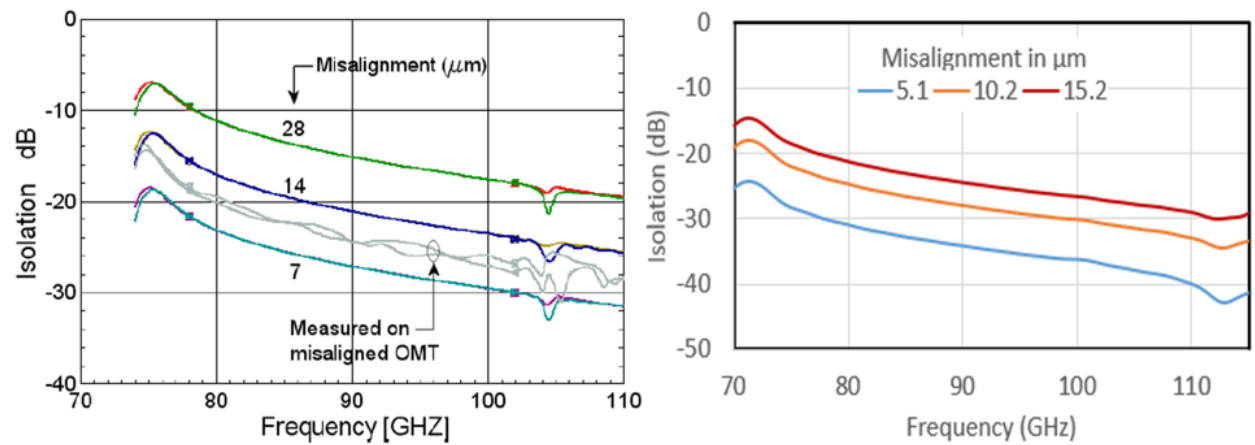
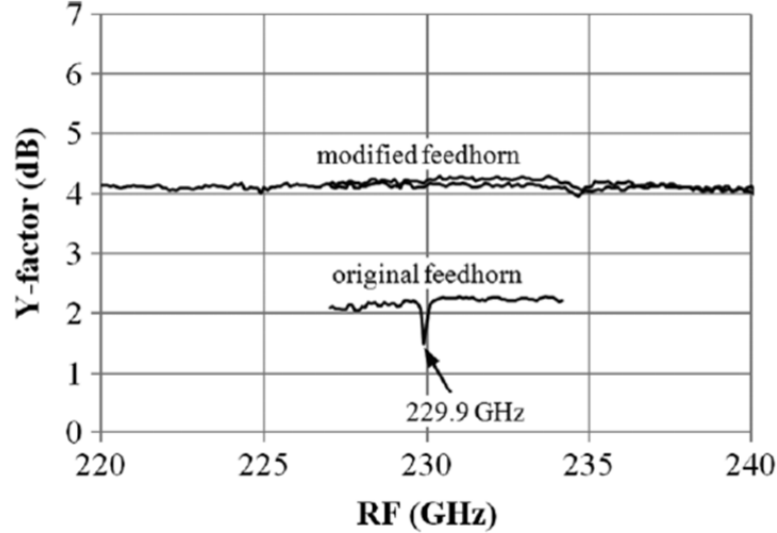


Fig. 3.3 Effect of misalignment between the block halves on polarization isolation for the WR-10 scale model. Left: Original Dunning OMT design, simulated and measured results. Right: Modified Dunning OMT, simulated results only. Note the difference in the misalignment scales of the two graphs.

Following a suggestion of Neal Erickson of UMass, we have modified the OMT to be less sensitive to alignment between the block halves. This is shown in Fig. 3.3 (right). The improvement in polarization isolation is about 3 dB within the 1.3:1 frequency band. It is believed that the bandwidth of this OMT could be increased further, and we plan to explore this and continue our collaboration with Erickson in the next phase of this work.

#### *Trapped mode*

Small peaks in the noise temperature of some Band-6 receivers are observed near 230 GHz and 256 GHz. These were identified by Morgan and Pan [3.2] as trapped mode resonances in the OMT and between the OMT and feed horn. Fig. 3.1 shows such a resonance before and after modification of a feed horn to eliminate the trapped mode. A small change in the OMT-feed horn interface removes this resonance.



**Fig. 3.1** Measured response of an ALMA Band 6 receiver receiver showing the 230 GHz resonance with the original and modified feedhorns. The multiple curves correspond to overlapping RF coverage with different LO frequencies. Vertical offset is added for clarity. From Morgan and Pan [3.2].

## **4. Discussion and conclusion**

### *SIS junction development*

SIS mixers using Nb/Al-AIN/Nb junctions have been shown to have noise performance comparable to those with the standard Nb/Al-AIOx/Nb junctions. This opens the way to a new generation of SIS mixers for ALMA Bands 3-10 with wider RF coverage and flatter noise temperature across the band. The higher critical current density possible with an AIN tunnel barrier allows smaller SIS junctions with lower capacitance.

SIS junctions with one or both electrodes of NbTiN will allow substantial improvement of receiver noise temperatures in ALMA Bands 9 and 10. With both electrodes NbTiN, AIN was deposited using Reactive Bias Target Ion Beam Deposition (RBTIBD). The resulting NbTiN/AIN/NbTiN SIS junctions had a gap voltage close to 5 mV (cf. ~2.8 mV for Nb/Al-AIOx/Nb junctions). Further work is planned in which AIN will be deposited on heated NbTiN films. This is expected to improve the quality (leakage current) of the all-NbTiN junctions with high critical current density to that of the Nb/Al-AIN/Nb junctions with grown AIN tunnel barriers. (At the time of writing, funding to continue this work has not been forthcoming.)

### *Wideband balanced IF amplifiers*

The critical component of the 4-12 GHz balanced amplifiers is the superconducting quadrature hybrid on a small chip. These quasi-lumped-element circuits have been successfully made using three layers of Nb separated by thin films of SiO<sub>2</sub>. We have collaborated with Low Noise Factory to combine two of their MMIC amplifier chips with a pair of the superconducting hybrids and a mixer bias chip in a small package. The power dissipation will be within the 8.5 mW limit for IF preamps on ALMA. A quote has been received from LNF and we are awaiting NRAO management approval to place the order. This work will be continued under a new ALMA Study grant.

### *OMT and feed horn*

The Dunning orthomode transducer is extremely sensitive to misalignment between the two block halves. Following a suggestion of N. Erickson of U. Mass, we have modified the original design to reduce that sensitivity. We plan to continue working with N. Erickson to further reduce the sensitivity to misalignment while increasing the bandwidth.

In some of the present Band-6 receivers there is a small suckout near 230 GHz. The cause of the suckout has been identified and the OMT-horn interface will be modified in the new design to ensure better alignment between the horn and OMT and eliminate the trapped mode.

### **References:**

- [1.1] T. W. Cecil, M. Cybrey, R. Matthews, A. W. Lichtenberger, "Development of Nb/Al-AlN/NbTiN SIS Junctions," IEEE Transactions on Applied Superconductivity, Vol 19, Issue 3, pp. 409-412, June 2009.  
<http://ieeexplore.ieee.org/stamp/stamp.jsp?tp=&arnumber=5153065>
- [2.1] A. R. Kerr, J. Effland, A. W. Lichtenberger, and J. Mangum, "Towards a Second Generation SIS Receiver for ALMA Band 6," ALMA Development Study Report, 23 March 2016,  
<https://science.nrao.edu/facilities/alma/alma-development-cycle4/2nd%20Gen%20Band%206%20Rcvr>
- [2.2] M. W. Pospieszalski, A. R. Kerr, J. Mangum, "On the Instantaneous SIS Receiver Bandwidth," ALMA Memo 601, 12 Oct 2016. <http://library.nrao.edu/public/memos/alma/memo601.pdf>
- [2.3] A. R. Kerr, "On the Noise Properties of Balanced Amplifiers," IEEE Microwave and Guided Wave Letters, vol. 8, no. 11, pp. 390-392, Nov. 1998.  
<http://ieeexplore.ieee.org/stamp/stamp.jsp?tp=&arnumber=736255>
- [2.4] Model CA7256D. MAC Technology Inc., Klamath Falls, OR, USA [Online]. <http://www.mactechnology.com>
- [2.5] A. R. Kerr, A. W. Lichtenberger, C. M. Lyons, E. F. Lauria, L. M. Ziurys, and M. R. Lambeth, "A Superconducting 180° IF Hybrid for Balanced SIS Mixers," Proc. 17 th Int. Symp. on Space THz Tech., Paris, pp. 29-32, May 2006. <http://www.nrao.edu/meetings/issst/papers/2006/2006029034.pdf>
- [2.6] C. M. Lyons, A. W. Lichtenberger, A. R. Kerr, E. F. Lauria, L.M. Ziurys, "A Nb-Based 180-Degree IF Hybrid for Balanced SIS Mixers," Applied Superconductivity Conference, Seattle, Aug 2006.  
<http://ieeexplore.ieee.org/stamp/stamp.jsp?tp=&arnumber=4277575>
- [2.7] G. L. Matthaei, L. Young, E. M. T. Jones, "Microwave Filters, Impedance-Matching Networks, and Coupling Structures," New York: McGraw-Hill, 1964.
- [2.8] A. R. Kerr, "Surface impedance of superconductors and normal conductors in EM simulators," Millimeter Array Memorandum 245, National Radio Astronomy Observatory, Charlottesville VA, rev. Jan. 1999.  
<http://library.nrao.edu/public/memos/alma/memo245.pdf>
- [2.9] A. R. Kerr and S.-K. Pan, "Design of planar image-separating and balanced SIS mixers," Millimeter Array Memo No.151, National Radio Astronomy Observatory, March 1996.  
<http://library.nrao.edu/public/memos/alma/memo151.pdf>
- [3.1] A. Dunning, S. Srikanth, and A. R. Kerr, "A Simple Orthomode Transducer for Centimeter to Submillimeter Wavelengths," Proc. 20th International Symposium on Space Terahertz Technology, 20-22 April 2009, pp. 191-194.  
<http://www.nrao.edu/meetings/issst/papers/2009/2009191194.pdf>
- [3.2] M.A. Morgan and S.K. Pan, "Graphical Prediction of Trapped Mode Resonances in Sub-mm and THz Networks," submitted to 23rd International Symposium on Space Terahertz Technology, Tokyo, 2-4 April 2012.  
<http://ieeexplore.ieee.org/stamp/stamp.jsp?tp=&arnumber=6422345>